



Aalborg Universitet

AALBORG UNIVERSITY  
DENMARK

## Control Principles for Island Operation and Black Start by Offshore Wind Farms integrating Grid-Forming Converters

Pagnani, Daniela; Kocewiak, Łukasz; Hjerrild, Jesper; Blaabjerg, Frede; Bak, Claus Leth

*Published in:*  
24th European Conference on Power Electronics and Applications, EPE 2022 ECCE Europe

*Publication date:*  
2022

*Document Version*  
Accepted author manuscript, peer reviewed version

[Link to publication from Aalborg University](#)

*Citation for published version (APA):*  
Pagnani, D., Kocewiak, Ł., Hjerrild, J., Blaabjerg, F., & Bak, C. L. (2022). Control Principles for Island Operation and Black Start by Offshore Wind Farms integrating Grid-Forming Converters. In *24th European Conference on Power Electronics and Applications, EPE 2022 ECCE Europe* IEEE.  
<https://ieeexplore.ieee.org/document/9907081>

### General rights

Copyright and moral rights for the publications made accessible in the public portal are retained by the authors and/or other copyright owners and it is a condition of accessing publications that users recognise and abide by the legal requirements associated with these rights.

- Users may download and print one copy of any publication from the public portal for the purpose of private study or research.
- You may not further distribute the material or use it for any profit-making activity or commercial gain
- You may freely distribute the URL identifying the publication in the public portal -

### Take down policy

If you believe that this document breaches copyright please contact us at [vbn@aub.aau.dk](mailto:vbn@aub.aau.dk) providing details, and we will remove access to the work immediately and investigate your claim.



Aalborg Universitet

AALBORG UNIVERSITY  
DENMARK

## Control Principles for Black Start and Island Operation of Offshore Wind Farms integrating Grid-Forming Converters

Pagnani, Daniela; Kocewiak, Lukasz; Hjerrild, Jesper; Blaabjerg, Frede; Bak, Claus Leth

*Published in:*  
EPE 2022 ECCE Europe

*Publication date:*  
2022

*Document Version*  
Accepted author manuscript, peer reviewed version

[Link to publication from Aalborg University](#)

*Citation for published version (APA):*

Pagnani, D., Kocewiak, L., Hjerrild, J., Blaabjerg, F., & Bak, C. L. (Accepted/In press). Control Principles for Black Start and Island Operation of Offshore Wind Farms integrating Grid-Forming Converters. In *EPE 2022 ECCE Europe* (pp. 1-11)

### General rights

Copyright and moral rights for the publications made accessible in the public portal are retained by the authors and/or other copyright owners and it is a condition of accessing publications that users recognise and abide by the legal requirements associated with these rights.

- Users may download and print one copy of any publication from the public portal for the purpose of private study or research.
- You may not further distribute the material or use it for any profit-making activity or commercial gain
- You may freely distribute the URL identifying the publication in the public portal -

### Take down policy

If you believe that this document breaches copyright please contact us at [vbn@aub.aau.dk](mailto:vbn@aub.aau.dk) providing details, and we will remove access to the work immediately and investigate your claim.

# Control Principles for Island Operation and Black Start by Offshore Wind Farms integrating Grid-Forming Converters

Daniela Pagnani<sup>\*,♦</sup>, Łukasz Kocewiak<sup>\*</sup>, Jesper Hjerrild<sup>\*</sup>,  
Frede Blaabjerg<sup>♦</sup>, Claus Leth Bak<sup>♦</sup>

<sup>\*</sup>ØRSTED

Gentofte, Denmark

[{DAPAG, LUKKO, JESHJ}@orsted.com](mailto:{DAPAG, LUKKO, JESHJ}@orsted.com)

<sup>♦</sup>AALBORG UNIVERSITY

Aalborg, Denmark

[{fbl, clb}@energy.aau.dk](mailto:{fbl, clb}@energy.aau.dk)

## Keywords

«Wind energy», «Batteries», «Grid-forming converters», «Modelling», «Design».

## Abstract

In this paper, control principles to perform black start services by offshore wind farms (OWFs) integrating grid-forming (GFM) control are presented. The strategy consists in exploiting a GFM battery energy storage system (BESS) to provide black start services by an OWF equipped by grid-following wind turbines. Controller modelling and operation methodology are explained. In order to show the proposed control and operation principles, the analysis is implemented on the CIGRE Working Group C4.49 benchmark, which could resemble modern large OWFs in the United Kingdom, such as Hornsea Project 1 and 2. Analysis simulations in the software PSCAD show the success of the proposed strategy.

## Introduction

Today's power system is rapidly changing with the phaseout of synchronous generators (SGs) and the increasing deployment of renewable-based resources. SGs provide many grid services, in particular, the black start is of main interest for this study. Between renewable energy sources, a number of large offshore wind farms (OWFs) have been developed recently, especially in Europe and China and many more are under development worldwide, as seen in Fig. 1, where an overview of the total offshore wind installations by country is shown [1]. Despite the impact of COVID-19 pandemic challenging the normal development of operations, offshore wind had its second-best year ever in 2020 [1]. In the case of OWFs, black start represents a new service to be performed, as current wind turbines (WTs) are based on grid-following (GFL) converters that do not have the capability to work unless connected to the grid or an auxiliary SG. Black start has a specific grid code requirement to fulfil and some transmission system operators, e.g., National Grid Electricity System Operator (NGESO) in the United Kingdom, are investigating the implementation of this service by renewable energy sources [2, 3]. The most important requirement is the self-start capability (i.e., energisation without relying on the transmission grid). This implies equipment able to self-start, which can be achieved by grid-forming (GFM) converter control, to avoid relying on SGs and ultimately facilitate a 100% renewable-based black start strategy. Another requirement concerns the service availability (i.e., the ability to deliver black start services over a year), which must be a minimum of 90% for NGESO. This may be challenging for renewable energy, due to the intrinsic non-dispatchable nature of the source. Thus, the integration of an energy storage system seems advantageous.

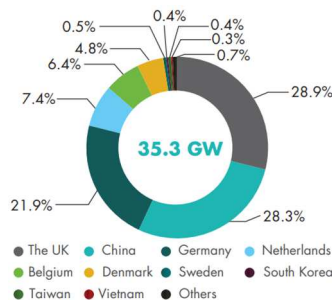


Fig. 1: Total offshore wind installations by country [1].

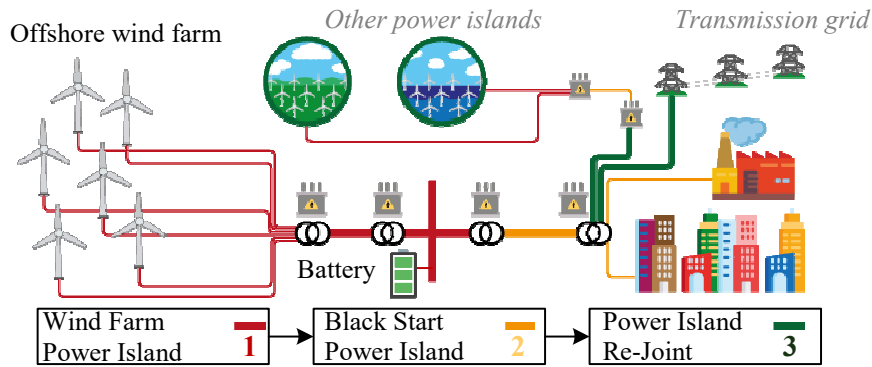


Fig. 2: Schematic of the proposed system consisting of an offshore wind farm equipped with a battery and the stages comprised in a black start process.

This paper primarily addresses the integration of a battery energy storage system (BESS) equipped with GFM control into an OWF to perform black start services, which has to work in parallel with GFL WTs. The system is shown in Fig. 2, where the BESS is a large, centralised unit located in the onshore substation of the OWF.

The integration of a BESS into renewable-based power plants and microgrids has been investigated in different studies, as able to increase flexibility by bidirectional active power exchange [4]. Moreover, such a storage system can provide black start, inertial and frequency regulation services [5]. A large STATCOM integrated with battery storage was initially proposed in [6], to enable the black start capability of OWFs. The STATCOM functionality provides fast and dynamic reactive power management and hence contributes to voltage regulation. These devices have been commercialised by the name of IBESS and or/ e-STATCOM [7-9].

The practical feasibility of successfully providing black start services from an OWF still has to be proven, as no OWF is currently able to restore a black grid. Therefore, more research needs to be conducted. Some literature around the main topic can be found in [7, 8, 10], where some discussions are made around OWF system configuration and control for a black start. However, little research is found, which discusses the whole black start procedure starting with an OWF with integrated BESS and addresses the control principles behind this hybrid power plant.

This paper analyses the implementation of a hybrid GFM-BESS+GFL-WT control system shown in Fig. 2. Furthermore, simulations in PSCAD are performed on an OWF model inspired by the CIGRE WG C4.49 benchmark, to validate the designed system and present the success of the black start procedure.

## Grid-Forming Control Applied to Black Start and Island Operation

GFM converter control is a concept that has been developed extensively in the last decades and represents a novel way of integrating grid-connected converters [11]. For example, GFM converters in photovoltaic applications in microgrids have been available since around 2000 in the multi-kW range and around 2010 in high power applications (>MW) [12]. More recently, their application has been expanded to different technologies, i.e., BESSs and WTs, and several GFM strategies have been developed, e.g., droop-based control, virtual synchronous machine, power synchronisation control (PSC) [10, 13]. The designation *grid-forming* is used as an umbrella term for any inverter controller that regulates its internal voltage phasor and can be the only source in the grid to which it is connected, or it can coexist with other GFL and GFM inverters, as well as SGs [14]. In the literature, sometimes the latter converter (i.e., GFM) is defined as a grid-supporting voltage source [11, 15]. A universal definition is yet to be agreed upon. However, the main concept represents a controller for inverters in grid applications that do not necessarily need a voltage vector reference, e.g., as the phase-locked loop (PLL) does, to be the main loop to create its voltage phase reference and synchronise itself to the grid but it can create its own. Therefore, they are in contrast with GFL, where the need for an energised grid with a voltage vector to follow is indispensable for the controller. This is important with the operation of black start, as there is the need for a converter which can form the voltage without an existing grid, along the lines of a traditional SG. Additionally, it needs to have the capability to self-start. Thus, the concept of a GFM converter is a necessary but not sufficient condition when discussing black start by OWFs.

The interesting GFM converter concept for this research is applied to the converter that can both self-start and form its own voltage vector in the instance of the grid.

### Selected Grid-Forming Control

In this paper, the GFM control strategy selected is implemented in the inverter of a large-scale BESS integrated into the onshore substation of the OWF as per Fig. 2. The GFM control applied is based on PSC with virtual inertia and damping, as shown in Fig. 3. This has been chosen as it is an established control topology, where the additional contribution of inertia and damping can be implemented.

For GFM purposes, the PSC was proposed in [16] to emulate the synchronisation mechanism based on transient power exchange seen in SGs. Thus, the resemblance with the swing equation of synchronous machines. PSC has been initially designed to be implemented in high-voltage direct current (HVDC) transmission to tackle weak grid conditions. In this GFM application, the frequency deviation  $\Delta\omega$ , corresponds to the deviation in active power  $\Delta P$ , and it is given in Eq. 1.

$$\Delta\omega = \frac{1}{2Hs + \frac{k_d s}{\omega_d + s} + k_g} \Delta P \quad (1)$$

where  $H$  indicates the inertia constant as defined in the conventional power system, which tends to resist the frequency deviations. The damping parameter  $k_d$  will be able to damp out the high-frequency oscillations if any in the power deviation. Furthermore, the reciprocal of the parameter  $k_g$  indicates the droop frequency response of the BESS. In this study, 1.6% frequency regulation droop is used as in [7].

### Implemented Control Principles

In this section, the modelling and design of the system in this proposed OWF will be shown. Each controller will be presented, having the GFM controller first, and the GFL controller second. This will show the applied control principles for such a system and some key differences in the application of GFM and GFL control for black start purposes.

The converters are implemented using the space vector notation and an average model in the  $dq$ -frame rotating at rated frequency, in combination with proportional-integral (PI) controllers. These are universally known because of their flexibility combined with the relatively easy tuning. Due to the capabilities of the integral action to estimate load disturbance, a certain stability margin in the closed loop is obtained. Several techniques can be applied given the need for converter control modelling for design purposes. One of the most popular approaches is Laplace domain ( $s$  domain) analysis, which can be done using transfer functions. This method is based on the transfer function analysis, which relates the output to the input, which for this type of study are the measured variable and the reference variable. The analysis is based on the models in the  $s$ -domain, with an assumption that the controller sampling rate is fast enough and the impact from discretisation can be neglected. It is assumed that all the power needed during the operation can be extracted from the DC link, for simplification. This means that the DC-link voltages of the converter-based resources, i.e., BESS and WTs, are constant.

### Grid-Forming Battery Energy Storage System Modelling and Design

The selected GFM controller for the BESS is the PSC with VSM variation, i.e., additional virtual inertia and damping terms, shown in Eq. 1, and the BESS parameters are adapted from [8].

A modular multilevel converter (MMC) type of structure is chosen for the large rating (>100 MVA) needed for this application. A single-line diagram of the BESS and its controllers is shown in Fig. 3. Thanks to the MMC internal filters, no large filters are needed at the inverter output, thus only an L filter is shown in the diagram. MMCs can reach high voltage levels, therefore the inverter output voltage is 33 kV. In order to connect the BESS to the onshore bus of the selected OWF, a step-up transformer is needed to reach the 220-kV level. The sizing of the BESS is not included in this study, where it is assumed that the BESS is large enough to perform the black start. However, the base values for the converter are needed, thus it is assumed that the active power rating of the BESS is 50 MW/100 MWh, while the reactive power rating (STATCOM capability) is 100 MVar. Thus, the apparent power is assumed as 112 MVA. This has been inspired by [7].

The GFM controller is made of two parts: (i) the power synchronization loop (PSL) and (ii) the alternating voltage controller. Its principle is based on setting the converter voltage as  $\mathbf{v}_c = V e^{j\theta}$ .

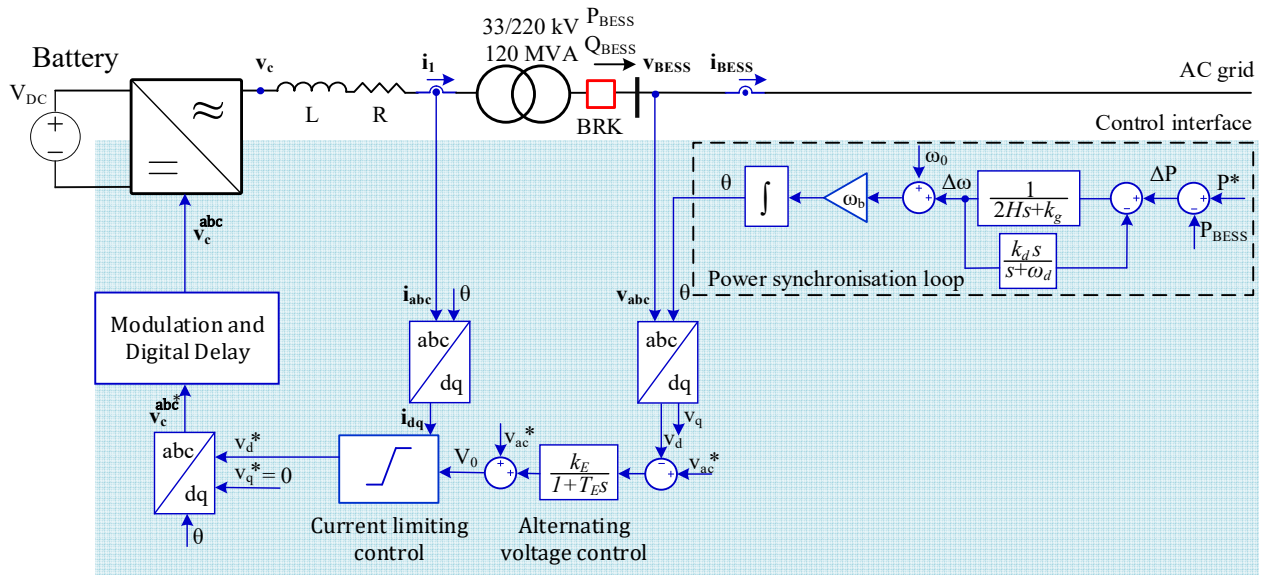


Fig. 3: System configuration and control structure for the grid-forming battery system implemented in the analysis.

### Grid-Following Wind Turbine Modelling and Design

Fig. 4 shows the control strategy implemented for the GFL WTs. It is assumed that this is a typical two-level converter rated at 12 MW. The GFL control is using standard cascaded control loops, the inner loop controlling the converter side current, whereas the outer loop controls the active and reactive power generated by the WT. Since a GFL WT is considered, a PLL is applied to provide grid synchronisation. It is assumed an LCL filter is used, where the grid-side inductance is represented by the 0.69/66 kV transformer. Due to the resonance characteristic of this converter, an active damping term based on capacitive current is implemented in the current control loop. The system parameters are selected and adapted from [17].

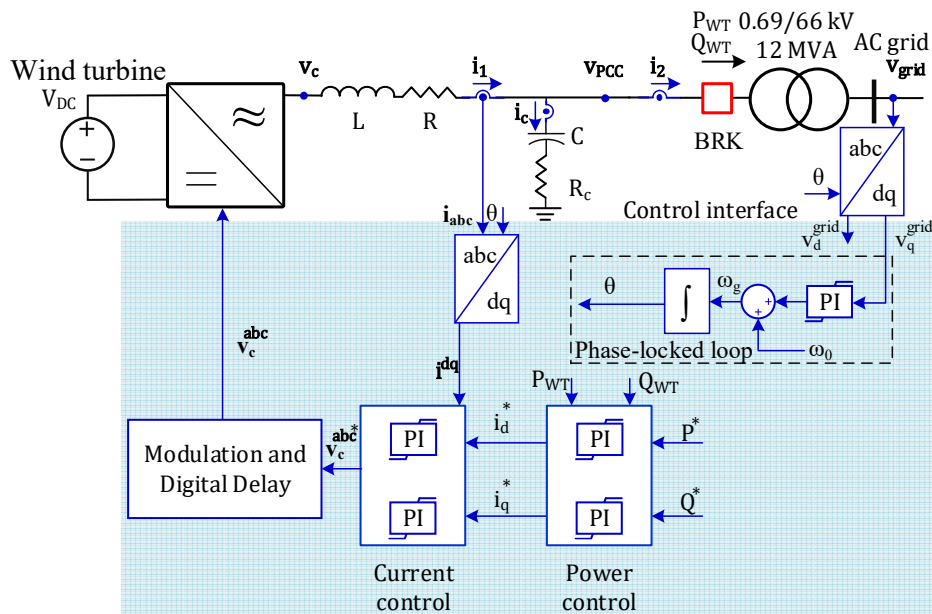


Fig. 4: System configuration and control structure of the grid-following wind turbine used in the analysis.

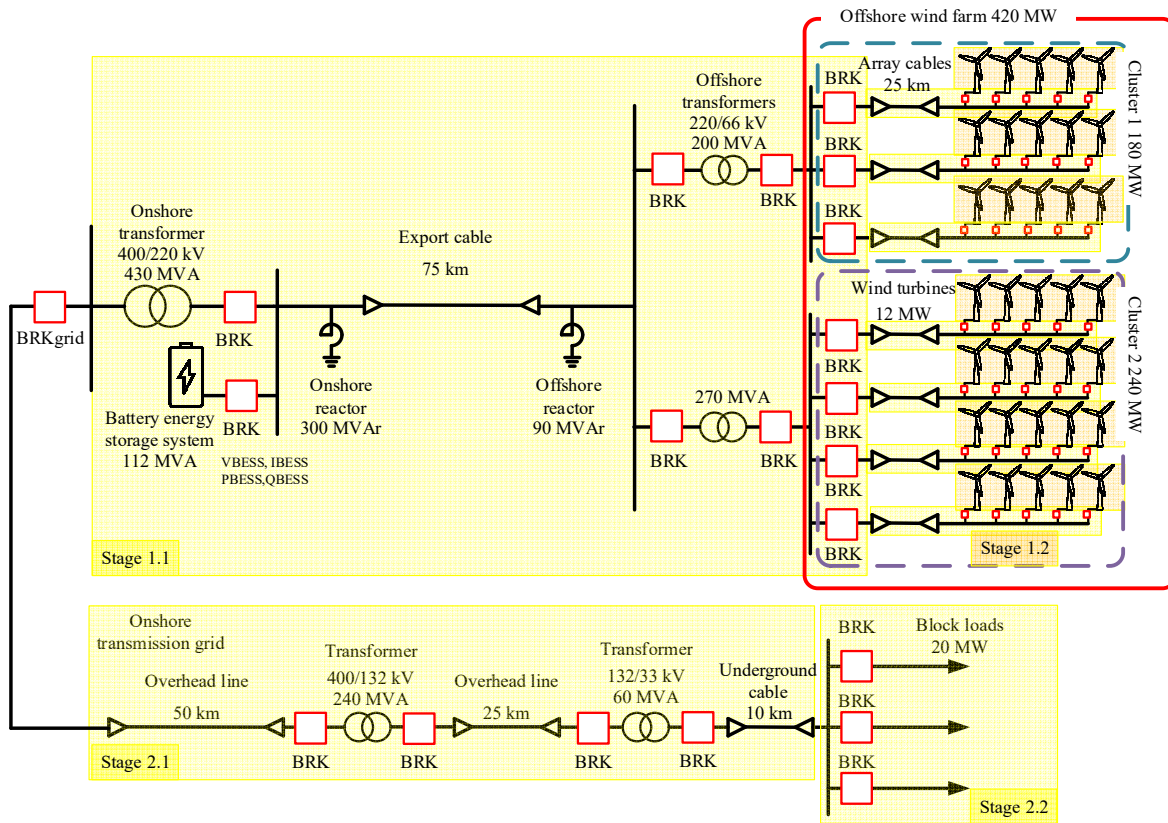


Fig. 5: Diagram of the study case based on the CIGRE WG C4.49 benchmark (BRK = circuit breaker) and onshore transmission network, where the energisation stages are highlighted.

## Simulation Results of Black Start and Island Operation

An OWF system inspired by the benchmark proposed by CIGRE WG C4.49 has been implemented in PSCAD, which is shown in Fig. 5.

A black start procedure implemented by an OWF can be said to be comprised of different stages, going from a state of no power to a state of restored normal operation for the power system, as shown in Fig. 2 [3]. It is assumed that the OWF is completely shut down following a blackout of the transmission grid or an event of similar impact. Moreover, the OWF is islanded, i.e., disconnected from the main grid. It is imagined that an assessment of the possible damage to the OWF following the blackout is performed, and the wind farm is able to continue without any issues. Once that is cleared, the next step for the OWF operator is to establish the energisation plan and capacity, which in this case means to assure the reserved BESS capacity for black start and the wind prediction. After that, the OWF is ready to receive the signal from the TSO to start the black start procedure. When using an OWF as a black start source, the first stage represents the energisation of the wind farm in island operation, i.e., working as a Wind Farm Power Island. Once the island is energised and stable, the energisation of the onshore transmission grid and the energising of the block loads can start and thus form a Black Start Power Island. This is also a challenging operation, as the transmission grid itself consists of many transmission lines and transformers with little or no load, determining a grid high harmonic impedance at low frequencies and little damping. Additionally, the main purpose is to energise large block loads ( $\geq 20$  MW) in one single switching operation. After the energisation of a part of the system, the synchronisation with other power islands in the system has to take place until the full system is synchronised and restored. This final stage is referred to as Power Islands Re-Joint. These stages are shown in Fig. 2, and more in details in Fig. 6 [3]. As they have different characteristics, they will be analysed separately.

### System Configuration

The OWF system is based on the CIGRE WG C4.49 benchmark, where a large BESS has been integrated into the study case [17]. This is depicted in Fig. 5.



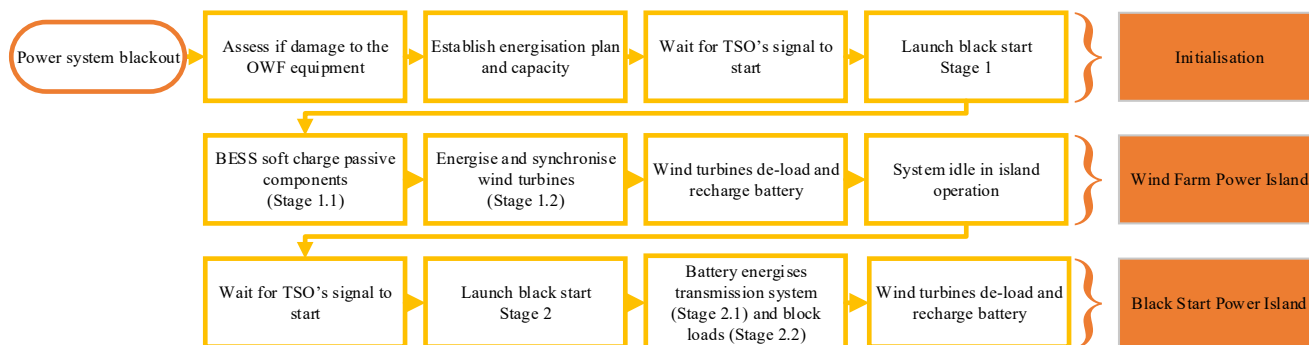


Fig. 6: Flowchart schematising the main steps of the implemented black start procedure.

The rated OWF active power is 420 MW and comprises 35 WTs rated at 12 MW. The export cable is a long, 220-kV high-voltage alternating current (HVAC) cable, which has 300 Mvar shunt compensation at the onshore end and 90 Mvar at the offshore end. The export cable length has been assumed as 75 km as it is considered a good scenario to represent modern, large OWFs which are far from shore such as the Hornsea projects in the UK, but without necessitating a midpoint reactive compensation station. The export cables comprise 35-km long land cables and 40-km long sea cables. These are modelled by a frequency-dependent model in PSCAD since it is useful for studies wherever the transient behaviour of the cable is relevant. The export cable is connected to the onshore substation where the BESS is located, together with a 400/220 kV, 420 MVA onshore transformer. In all the transformers, the saturation characteristics have been modelled, in order to show the impact of the phenomenon.

Offshore, there are 35 WTs rated at 12 MW and arranged in seven strings, each string having five WTs. These strings are collected in two WT clusters, one having three strings and the other having four strings. Two 220/66 kV transformers connect the export system to the collection system with a rated power equal to 200 and 270 MVA respectively for the two WT clusters. The 66-kV collection system is made of two different types of three-core cables, respectively 500 mm<sup>2</sup> and 150 mm<sup>2</sup> submarine cables. The three first WTs on the feeder are connected via the 500 mm<sup>2</sup>, while the last two apply the 150 mm<sup>2</sup> cables. It is assumed that the cable length between WTs is constant and equal to 5 km. These two WT clusters have been aggregated in order to save computational time for the simulation, where they are modelled as seven individual feeders with five aggregated WTs each. The aggregated collection cables are modelled via the equivalent T model, while the WT ratings are correspondingly scaled up. An advantage of this aggregated model is lower computational time and speed up the simulation execution. However, this can cause a misrepresentation of the energisation phenomenon, since large groups of WTs are energised at the same time, while in reality it will be one at the time. Accordingly, it can be discussed that the success of this energisation in this simulation, therefore, is harder to achieve as a larger unit is energised at once. In contrast, the process is made of more and smaller steps in real life.

On the onshore side, it is assumed that the black start provider may have to energised block loads which are connected via a series of lines and transformers and at lower voltage level. Thus, the OWF+BESS system is connected onshore to a radial network which starts with a 50 km long overhead line at 400-kV level, which in turns is connected to a 400/132 kV transformer. This is in turn connected to a shorter overhead line (20 km) and another step-down transformer (132/33 kV). Finally, a 10 km long underground cable connects the system to three block loads each of 20 MW. This is assumed as a demonstration of the black start capabilities of the system, but it is assumed that a higher number of block loads can be covered by the OWF capacity when wind is available for the necessary period of time. This representation of the onshore grid, with both block loads and lines and transformers, is chosen to challenge the islanded network which has to comply with the requirements for black start, i.e., minimum 20 MW block loads capability and 100 Mvar reactive power capability [2, 3].

### 1st Stage: Wind Farm Power Island

The first step in the black start of the onshore transmission grid is the black start of the BESS and consequently of the OWF grid, in order to establish a Wind Farm Power Island. The steps for this to happen are: (i) energisation of the BESS and passive components, (ii) energisation and synchronisation



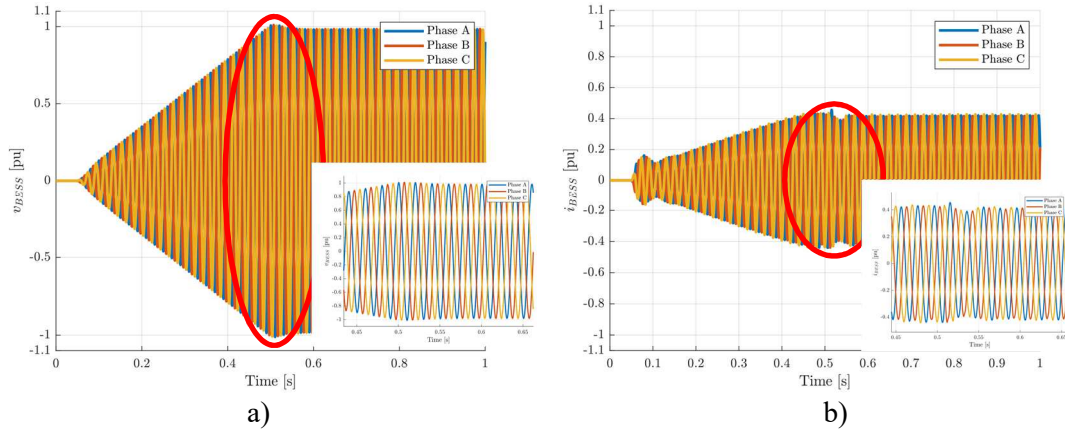


Fig. 7: Simulation results from the soft charge of the wind farm passive system in Fig. 5 by the grid-forming battery measured at its point of connection: a) Generated battery voltage, b) Generated battery current.

of the WTs, (iii) de-loading and recharging of the BESS by the WTs to compensate for the system losses. Being the BESS the largest active component in the system (50 MW against 12 MW), and being a dispatchable type of source, it is decided that this component will be the one used for the single energisation steps alone. In this way, we can ensure a more resilient system by avoiding multiple converter actions and their interactions. Thus, the BESS is always acting first and after a new steady state is achieved, it can be recharged by the WTs. This will allow the BESS to be fully recharged and idle till the next step can be performed. The procedure is illustrated in the flowchart in Fig. 6. The offshore grid can be energised in two ways: by hard switching or by soft charging (Stage 1.1). Hard switching is defined as performing the several switching operations for one component at the time after the BESS is self-energised and runs at 1 pu voltage. Inrush currents and temporary overvoltages when the BESS is connecting to the offshore grid are to be expected. On the other hand, by using soft-charging, all the circuit breakers in the OWF grid (without including the WTs) are connected and the voltage is slowly ramped up from 0 to 1 pu. Thus, the transient currents can be avoided to a large extent by decreasing the voltage ramp rate  $\frac{dv}{dt}$ . In this simulation study, the BESS voltage is ramped up from 0.0 to 1.0 pu in the period from 0.05 s to 0.5 s, while all the breakers shown in Fig. 5 are closed, with the exception of the breaker going to the onshore transmission network (BRKgrid in Fig. 5). Both the current and the voltage increase smoothly, and they remain balanced throughout the soft-charging process as shown in Fig. 7, where the voltage  $v_{BESS}$  and the current  $i_{BESS}$  are measured at the BESS converter terminals. This energises the onshore transformer, the export cable system with reactive power compensation, offshore transformers and the collection grid, including the WT transformers, and this is done in order to avoid a further switching operation. In general, the energisation of WTs starting from their transformers could likely cause sympathetic inrush due to their close electrical distance. Having

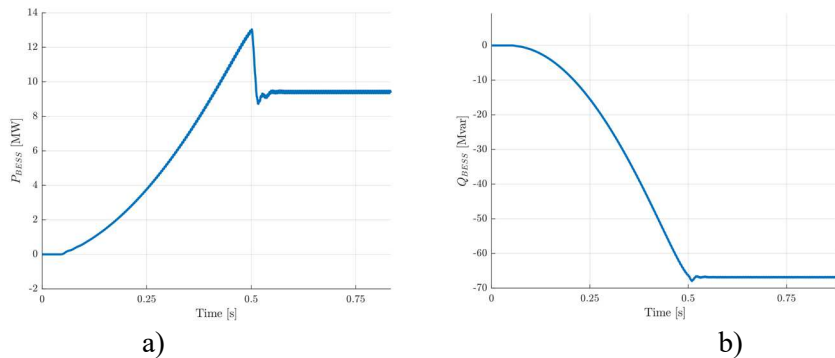


Fig. 8: Simulation results from the soft charge of the wind farm passive system in Fig. 5 by the grid-forming battery measured at its point of connection: a) Active power, b) Reactive power.

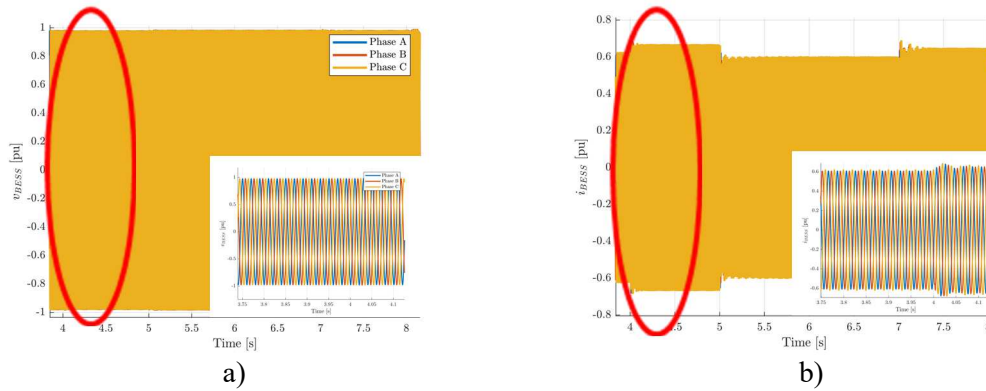


Fig. 9: Simulation results from the energisation and synchronisation of the first (at 4 s) and second (at 7 s) group of wind turbines in Fig. 5 by the grid-forming battery measured at its point of connection: a) Generated battery voltage, b) Generated battery current.

the BESS soft charging these components will avoid this type of drawback. During Stage 1.1, shown in Fig. 8, the BESS supplies the maximum active power of 12.95 MW, while it absorbs the maximum reactive power of 67.55 Mvar, which is generated by the high voltage export cables. This is the excess reactive power considering that all the shunt reactors in the OWF are connected. In steady state, at 0.6 s, the BESS supplies 9.50 MW and absorbs 66.85 Mvar, as shown in Fig. 8. The BESS is controlled to regulate its terminals at the high-voltage side of its transformer, and this is 1.05 pu after the soft charging process. Thus, the BESS absorbs this large amount of reactive power, i.e., over 65 Mvar to decrease its voltage. It can be seen that the active power required for energising the offshore grid is not substantial (but at the same time not negligible), while the BESS unit has to handle a large amount of reactive power which fluctuates between the reactive components in the system, especially the export cable. Therefore, the STATCOM capability is implemented. The next step is the energisation and synchronisation of the WTs (Stage 1.2). In this simulation, the five WTs included in one string are modelled as a single unit, and thus energised as they were energised at the same time. However, in real operations, one WT will be energised at the time. From the electrical point of view, the energisation of the WT unit starts when the voltage is sensed at the low-voltage terminal of its transformer, as seen in Fig. 4. After this, it is assumed that the WT starts powering its auxiliaries and can start operation at zero power, deblocking its converter and working in standalone mode for a brief period of time before its breaker is closed. During this short time window, the converter is already synchronised to the grid via its PLL, and once the converter is deblocked and the breaker closed, the WT is fully synchronised to the main wind power island. The first WT group, which is an aggregate of five WT units, is synchronised at 4 s, while the second group is connected and synchronised at 7 s, as shown in Fig. 9. The connection of the WT strings is made in succession with an interval of 3 s between each other. This is sufficient time to see the new steady state before the connection of the new group of WTs. It can be seen that a transient disturbance arising due to the connection of the WT units. From the BESS side, there is a momentary increase of the injected current, which goes from 0.6 to 0.72 pu for 1 s, as seen in Fig. 9. This relatively small transient disturbance appears whenever a WT group is connected to the grid and are observed in the simulation study when the WT groups are connected as each group comprises an aggregation of multiple WT units. Thus, the resultant transient at 4 s is the consequence of the simultaneous connection of 5 WT units through a 60 MVA transformer, and an aggregated LC filter. At 22 s, the power reference of the first WT group is ramped up from 0.0 to 0.3 pu in 1 s. This is done assuming that the WTs can take on the active power losses of the system and re-charge the BESS. In response to the change in the reference, the output active power from the WT groups rises. The battery is thus charged by absorbing the active power produced by the WTs.

## 2<sup>nd</sup> Stage: Black Start Power Island

In this stage, the actual black start of the onshore transmission network is achieved. Once the Wind Farm Power Island is established and working stably, the OWF operator has to wait for instructions from the transmission system operator and be ready for energising block loads in the transmission grid, as shown

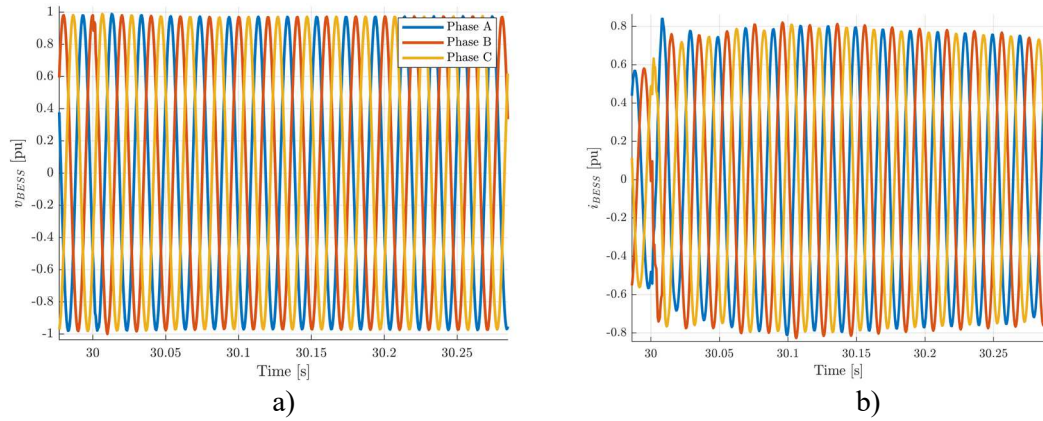


Fig. 10: Simulation results from the energisation of the first overhead line (at 30 s) in Fig. 5 by the grid-forming battery measured at its point of connection: a) Generated battery voltage, b) Generated battery current.

in the flowchart in Fig. 6. During this stage (Stage 2), the BESS, which is fully charged and de-loaded, is the one taking care of the extra active and reactive power loads of the transmission grid at first. It is only once the new components in the transmission grid are fully energised and stable, that the WTs will pick up the load and recharge the BESS. This cycle can be repeated for every block load to energise, and it is preferred in order to have the BESS as a single large unit to energise the large transmission system loads. To test the reactive power requirements for black start, the onshore grid has been modelled as a radial system where overhead lines, cables and transformers connect the block loads at 33 kV. This system is represented in Fig. 5 and it is made up of 50 km overhead line at 400 kV, connected to a 400/132 kV, 240 MVA transformer to another overhead line which is 25 km long. After that, there is a final 132/33 kV, 60 MVA transformer which connects to three 20 MW block loads.

The switching operation to energise the passive components of the transmission system (Stage 2.1) take place one component at the time and it is simulated by common switching operation, i.e., without advanced aids such as pre-insertion resistors or point of wave switching, and it causes heavy distortions to the BESS voltage and current waveforms. However, there are no overcurrents and overvoltages exceeding the 10% range, and the transients are all settled to steady state, thus the procedure is successful. The first overhead line is energised at 30 s, as seen in Fig. 11. This causes a large increase in the current (almost doubled), provided by the BESS, which goes from 0.5 to 0.9 pu, but this is still well below the limits. The transformer energisation is though the most problematic element to energise, as expected, and this is simulated at 33 s. The saturation phenomenon is known for causing inrush currents which are also seen here in Fig. 11, and last for several seconds. There is a rich harmonic component due to the switching and energisation of the transformer, which is relatively significant because the black start power island is very weak. However, it is damped due to the losses in the system.

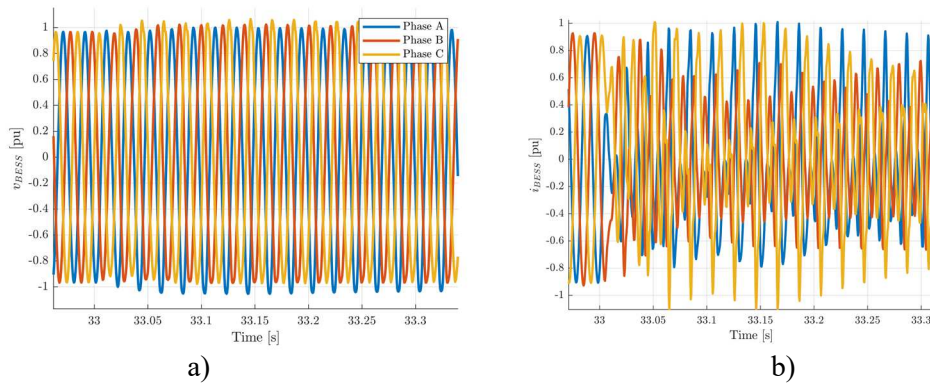


Fig. 11: Simulation results from the energisation of the first transformer at 33 s in Fig. 5 by the grid-forming battery measured at its point of connection: a) Generated battery voltage, b) Generated battery current.

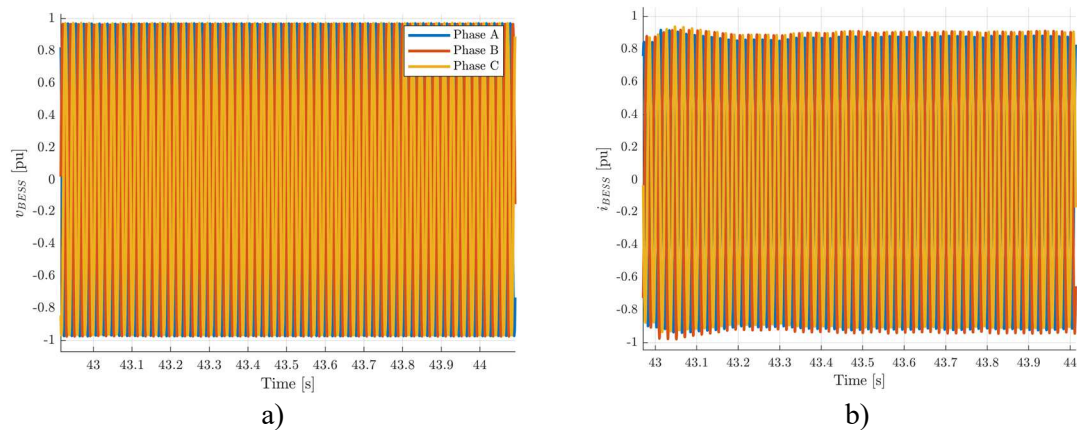


Fig. 12: Simulation results from the energisation of the block load at 43 in Fig. 5 by the grid-forming battery measured at its point of connection: a) Generated battery voltage, b) Generated battery current.

After connecting the remaining lines and transformer, the block loads are connected at 43 s, 45 s and 47 s, respectively, as shown in Fig. 12 (Stage 2.2). Compared to the energisation of the line, the block loads create negligible disturbance in the whole islanded grid. It is important for the WTs to support during the procedure as each block load draws a lot of energy and power.

The third and last stage of the black start procedure, i.e., the Power Island Re-Joint, is not addressed in this paper as it is directed, operated and controlled by the TSO. Thus, it is left as future work.

## Discussion and Conclusion

In this paper, the discussion is mainly focused on the control implementation and on its performance during the black start provided by a complex OWF system equipped with GFM BESS and GFL WTs. This is especially challenging as the system is very weak since it is working in no grid conditions, i.e., as an islanded network. However, the system is able to form an islanded network and connect different transmission components and block loads in the transmission grid.

It can be argued that a lot of energy is necessary in the overall black start restoration, and that could be challenging for a single GFM unit. Thus, the implementation of GFM controllers in the WTs could be a favourable future work for in order to support the BESS and accelerate the black start procedure, especially during Stage 1.2.

The proposed strategy for black start by an OWF with integrated battery is designed, implemented and simulated. The designed GFM control allows the system to react to the transient phenomena caused during the system energisation with stable performance and shows the challenges in implementing a black start strategy from a converter-based network and the principles to overcome them, such as the soft charge of the passive OWF system. From the practical point of view, it can be seen that the energisation of the reactive components in the onshore transmission grid is the most challenging part for the operation, due to the high reactive power load and transient operations involved in switching, such as inrush currents and temporary overvoltages.

It is shown how the selected BESS with GFM control can successfully perform this service together with a large OWF based on a generic benchmark system. When a specific power plant is designed for black start, only a detailed study will enable an assessment of the risks and an evaluation of the efficacy of the additional solutions to be provided.

## References

- [1] Global Wind Energy Council (GWEC), “Global Offshore Wind Report,” Brussels, 2021.
- [2] National Grid Electrical System Operator, “Restoration Services,” 21 January 2021. [Online]. Available: <https://www.nationalgrideso.com/sites/eso/files/documents/Appendix%201%20-%20Tech%20Requirements%20and%20Assessment%20Criteria.pdf>. [Accessed 1 June 2022].



- [3] D. Pagnani, Ł. H. Kocewiak, J. Hjerrild, F. Blaabjerg and C. L. Bak, "Integrating Black Start Capabilities into Offshore Wind Farms by Grid-Forming Batteries," in *IET Renewable Power Generation*, pp. 1-12, submitted 2021.
- [4] S. Saponara, R. Saletti and L. Mihet-Popa, "Hybrid Micro-Grids Exploiting Renewables Sources, Battery Energy Storages, and Bi-Directional Converters," in *Applied Sciences*, vol. 9, no. 22, pp. 1-18, 2019.
- [5] M. P. S. Gryning, B. Berggren, Ł. H. Kocewiak and J. R. Svensson, "Delivery of Frequency Support and Black Start Services from Wind Power Combined with Battery Energy Storage," in *Proc. 19<sup>th</sup> Wind Integration Workshop*, Online, pp. 1-10, 2020.
- [6] T. S. Sørensen, "Method for Black Starting an Electrical Grid". United States of America Patent 20200244070, 16 November 2018.
- [7] S. K. Chaudhary, R. Teodorescu, J. R. Svensson, Ł. H. Kocewiak, P. Johnson and B. Berggren, "Islanded Operation of Offshore Wind Power Plant using IBESS," in *Proc. 2021 IEEE Power & Energy Society General Meeting (PESGM)*, 2021, pp. 1-5, doi: 10.1109/PESGM46819.2021.9638226.
- [8] S. K. Chaudhary, R. Teodorescu, J. R. Svensson, Ł. H. Kocewiak, P. Johnson and B. Berggren, "Black Start Service from Offshore Wind Power Plant using IBESS," in *Proc. 2021 IEEE Madrid PowerTech*, 2021, pp. 1-6, doi: 10.1109/PowerTech46648.2021.9494851.
- [9] M. R. A. Wara and A. H. M. A. Rahim, "Supercapacitor E-STATCOM for Power System Performance Enhancement," in *Proc. 2019 International Conference on Robotics, Electrical and Signal Processing Techniques (ICREST)*, 2019, pp. 69-73, doi: 10.1109/ICREST.2019.8644388.
- [10] D. Pagnani, Ł. H. Kocewiak, J. Hjerrild, F. Blaabjerg and C. L. Bak, "Overview of Black Start Provision by Offshore Wind Farms," in *Proc. IECON 2020 The 46th Annual Conference of the IEEE Industrial Electronics Society*, 2020, pp. 1892-1898, doi: 10.1109/IECON43393.2020.9254743.
- [11] J. Rocabert, A. Luna, F. Blaabjerg and P. Rodríguez, "Control of Power Converters in AC Microgrids," in *IEEE Transactions on Power Electronics*, vol. 27, no. 11, pp. 4734-4749, Nov. 2012, doi: 10.1109/TPEL.2012.2199334.
- [12] E. Alegria, T. Brown, E. Minear and R. H. Lasseter, "CERTS Microgrid Demonstration with Large-Scale Energy Storage and Renewable Generation," in *IEEE Transactions on Smart Grid*, vol. 5, no. 2, pp. 937-943, March 2014, doi: 10.1109/TSG.2013.2286575.
- [13] D. Pagnani, F. Blaabjerg, C. Bak, F. Faria da Silva, Ł. Kocewiak and J. Hjerrild, "Offshore Wind Farm Black Start Service Integration: Review and Outlook of Ongoing Research," in *Energies*, vol. 13, no. 23, pp. 6286, 2020.
- [14] North American Electric Reliability Corporation (NERC), "Grid-Forming Technology," Atlanta, 2022.
- [15] A. Narula, M. Bongiorno, M. Beza and P. Chen, "Tuning and evaluation of grid-forming converters for grid-support," in *Proc. 2021 23rd European Conference on Power Electronics and Applications (EPE'21 ECCE Europe)*, 2021, pp. 1-10, doi: 10.23919/EPE21ECCEurope50061.2021.9570679.
- [16] L. Zhang, "Modeling and Control of VSC-HVDC Links Connected to Weak AC Systems," Royal Institute of Technology School of Electrical Engineering, Electrical Machines and Power Electronics, PhD Thesis, Stockholm, 2010.
- [17] Ł. Kocewiak, R. Blasco-Giménez, C. Buchhagen, J. B. Kwon, Y. Sun, A. Schwanka Trevisan, M. Larsson and X. Wang, "Overview, Status and Outline of Stability Analysis in Converter-based Power Systems," in *Proc. 19<sup>th</sup> Wind Integration Workshop*, Online, pp. 1-10, 2020.